Braun M, Ivañez I, Aranda-Ruiz J. Numerical analysis of the dynamic frequency responses of damaged micro-lattice core sandwich plates. The Journal of Strain Analysis for Engineering Design. 2020;55(1-2):31-41.

doi:10.1177/0309324719890958

Journal Title
XX(X):2–24

DOI: 10.1177/ToBeAssigned
www.sagepub.com/
SAGE

Numerical analysis of the dynamic frequency responses of damaged Micro-Lattice core sandwich plates

Matías Braun[1,2] and Inés Ivañez[3] and Josué Aranda-Ruiz[3]

Abstract

In this work, a numerical analysis of the dynamic frequency responses of sandwich plates with micro-lattice core is presented. The finite element analysis is implemented in the commercial software Abaqus/Standard, calculating the natural frequencies and eigenmodes of sandwich plates containing defects on the micro-lattice structure. In order to include the presence of defects an aleatory algorithm is developed in MatLab. The effect of the defects percentage, cell type, cell size and material on the frequency and modal responses of the sandwich plates are highlighted. Results show that the dynamic frequency response may be useful for analysing practical issues related to non-destructive damage identification of imperfections in the micro-lattice core of sandwich structures.

Keywords

Micro-Lattice, Sandwich Structure, Free Vibration Analysis, Finite Element Analysis

Prepared using sagej.cls *[Version: 2017/01/17 v1.20]*

Introduction

In the last decades, the use of composite sandwich structures extended to different engineering fields, such as aerospace, automotive, maritime and military [1–4]. This type of structures can be used in a variety of engineering problems, where the strength-to-weight ratio represent an important factor in the design process [5].

The sandwich structures with aluminium honeycomb core have been widely used in aerospace applications, as a result of their superior mechanical properties, such as specific stiffness and specific strength.

Nevertheless, the principal limitations of this kind of closed cells are associated with the gas and moisture retentions [6–8]. In order to solve these disadvantage many works have focused to optimise the design of open cells, such as the metallic lattice structures [9]. This work is centred on the study of open cell cores, in particular on a new micro-lattice (ML) core material manufactured using selective laser melting [10,11].

Many studies based on open cell geometries have greatly focused on predicting theoretically, numerically and experimentally the macroscopic stiffness and strength [12–16]. The scanning electron microscope images of the ML structures, presented in [12], showed that the structures are very complex and include imperfections which are semi-melted powders over the surface of micro-struts and variable diameters. Note that these defects affect the mechanical responses of the ML structure [17].

[1]Dpto. de Construcciones, Facultad de Ingeniería Universidad Nacional de La Plata, Buenos Aires, República Argentina.
[2] Consejo Nacional de Investigación Científicas y Técnicas (CONICET) CCT La Plata, Buenos Aires, República Argentina.
[3] Department of Continuum Mechanics and Structural Analysis, University Carlos III of Madrid. Avda. de la Universidad, 30. 28911 Leganés, Madrid, Spain.

Corresponding author:
Matías Braun, Calle 48 y 115 s/n, (B1900TAG) La Plata, Buenos Aires, República Argentina.
Email: matias.braun@ing.unlp.edu.ar

Prepared using sagej.cls

The presence of imperfections or damages in the structure produce changes in the stiffness that modify the vibration responses of the structure. Damage detection methods based on vibration can be performed as a real-time damage detection method to overcome the drawbacks of the common non-destructive testing (NDT) techniques. In the last three decades, a lot of researchers have focused on the study of damage detection based on vibration methods [18–23].

In the present study, to detect the presence of ML core defects a non-destructive damage detection method [24,25] based on vibration responses is analysed. The main objective of this work is to investigate the effect of ML imperfections on the modal dynamic responses of composite sandwich structures with ML core, using a finite element (FE) model implemented in Abaqus/Standard [26]. A MatLab algorithm was developed to include the aleatory presence of a certain percentage of imperfections on the lattice structure. Additionally, s statistical analysis of the results is presented, in order to define the dependence of the imperfection localisation on the vibration response. The influence of the damage percentage, cell type, cell size and material on the frequency and modal responses of sandwich plates is investigated. The obtained results show that the dynamic frequency responses are dependent on the imperfections (damage) percentage. Therefore, the use of vibration-based NDT methods allows to detect the presence of imperfections on the ML core of sandwich structures.

Geometrical and material properties

The geometry of the sandwich plate under study is shown in Fig. 1. The sandwich structure consisted of unidirectional composite face-sheets and ML core.

The composite face-sheets are made of CFRP with dimensions $75 \times 75 \times 1$ mm^3, while the core is made of 316L stainless steel [13] with

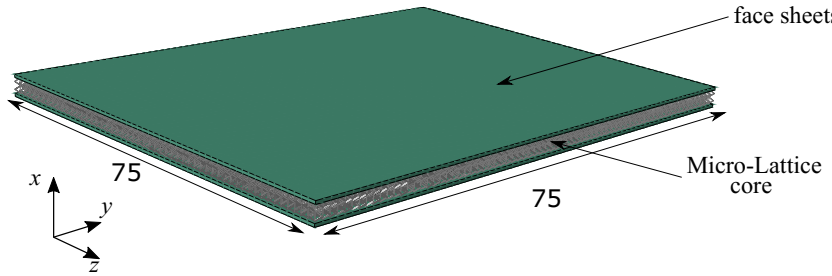

(a) Perspective view.

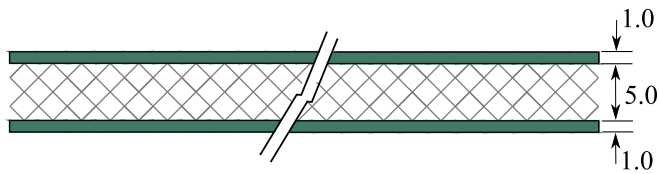

(b) Side view.

Figure 1. Geometry of the sandwich plate (all dimensions are in mm).

a thickness of 5 mm. There are no restrained degrees of freedom in the sandwich structure.

The material properties of the CFRP face-sheets used in the analysis are: $E_x = 140$ GPa, $E_y = E_z = 10$ GPa, $G_{yz} = 3.8$ GPa, $G_{xy} = G_{xz} = 4.6$ GPa, ν =0.25 and $\rho = 1650$ kg/m^3 [27].

It is considered that the ML bar structures exhibits a isotropic linear elastic behaviour with the following material properties: Young's Modulus $E = 140$ GPa, Poisson's ratio $\nu = 0.27$ and density $\rho = 7870$ kg/m^3 [13,28].

In this study, we considered two unit-cell topologies to the ML core: a body-centred cubic (BCC) and a same structure with vertical bar called BCC-Z. Fig. 2 shows a schematic representation of the two unit cells.

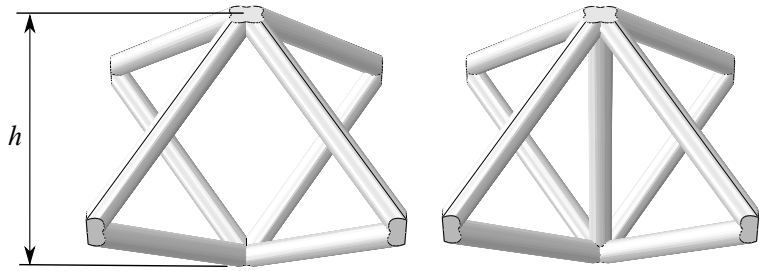

(a) BCC unit cell. (b) BCC-Z unit cell.

Figure 2. Configurations of the unit cells.

Numerical Model

The modelling and analysis of free vibration response of sandwich plates are carried out through the commercial FE code Abaqus/Standard[26]. The FE model consists of two parts: composite face-sheets and ML core.

The contact between the different parts is considered to be perfect and modelled using tie constraints, which are implemented in the Abaqus/Standard library[26]. These tie constraints apply a coupling to both displacements and rotations of each pair of interconnected elements of the structure.

The ML core is discretised using simple 2-node beam elements to represent the struts in the unit cell, according to the procedure presented by Smith *et al.*[29]. The geometry is simplified, so each strut was represented by a straight beam with a circular cross-section of diameter 0.20 mm.

In first place, a comparison between the numerical model in where three-dimensional elements have been used to mesh the ML core, and the numerical model in where the ML core is discretised using simple 2-node beam elements, is carried out, in order to validate the latter.

Furthermore, in order to validate the core discretization with beam elements, we implemented other FE model using a three-dimensional

elements to mesh the ML core. In this case, we used C3D8 elements (continuum three-dimensional reduced integration eight node elements) to mesh the ML structure.

The free vibration analysis is carried out using linear perturbation load step, obtaining the eigenvalues by means of Lanczos or subspace iteration methods[26]. Influences of imperfection existence on the modal behaviour are discerned by comparisons of dynamic response between a healthy (undamaged) sandwich plate, and sandwich plates containing imperfections in the ML core.

Fig. 3 presents a general view of FE mesh used to modelled the sandwich plate. The skins of the sandwich plate are discretised using 45000 C3D8R elements. The finite-element mesh of the ML core finally accepted due to convergence studies contained approximately 14398, 36846 and 48576 elements for cell sizes (h) of 2.5, 1.67 and 1.25 mm, respectively.

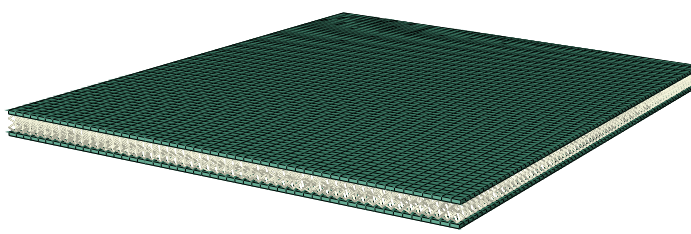

Figure 3. Typical mesh of FE model of the sandwich plate.

The presence of imperfections in the ML core are defined with an algorithm in the MatLab language. In order to define if the position of the imperfection affects the dynamic frequency response, we defined the imperfection with a random function. Note that it will be necessary to perform a statistical analysis of the obtained results.

Basically, the MatLab algorithm defines a random set of elements of the ML core. This set is incorporated within the Abaqus input file and is

assigned new material properties with null stiffness. Hence, these elements are fictionally vanished from the FE model.

Results and Discussion

In first place, a comparison between 3D continuum and beam elements is carried out, in order to validate the Beam model. Subsequently, a dynamic analysis of the undamaged sandwich structure is presented, showing the most predominant eigenmodes, and the values of the natural frequencies for different cell sizes and cell types. The values of the natural frequencies in the undamaged structure will be used to analyse the influence of damage on the dynamic responses of the sandwich plates.

Comparison between 3d continuum and beam elements

As mentioned above, in order to reduce the computational cost, a simplified model was developed. This simplified model replaces the three-dimensional elements of the core by simple 2-node beam elements to represent the struts in the unit cell.

With the aim of validate the Beam model, a comparison between the results obtained with both models was held. This comparison was made by calculating the natural frequencies of vibration, for the two unit cell topologies considered, obtaining in all cases the percentage error made with the simplified model. These results are shown in Table 1 and Fig. 4, considering the first 19 eigenmodes but avoiding those associated to natural frequencies unlikely to exist. These excluded modes correspond to the torsional modes, which have a complex shape and are difficult to implement in a vibration-based non-destructive testing method.

It can be seen that in all cases, the maximum percentage error does not exceed 7.2%. Taking into account all the analysed eigenmodes, the average error for the BCC unit cell is about 2.4%, while for the BCC-Z unit cell this average error increase up to 4.3%.

	BCC			BCC-Z		
Mode	3D [Hz]	Beam [Hz]	% Error	3D [Hz]	Beam [Hz]	% Error
1	2507.9	2470.7	1.5	2453.0	2436.6	0.7
2	3712.5	3654.7	1.6	3643.2	3629.6	0.4
3	5689.8	5673.4	0.3	5575.7	5621.0	0.8
4	8698.3	8870.5	2.0	8531.8	8817.9	3.4
5	9093.6	9328.2	2.6	8915.2	9268.0	4.0
6	9590.2	9820.3	2.4	9409.2	9772.9	3.9
7	10121	10344	2.2	9930.4	10291	3.6
8	11222	11482	2.3	11023	11453	3.9
14	15157	15717	3.7	14921	15888	6.5
15	15329	16083	4.9	15069	16102	6.9
16	15595	16111	3.3	15370	16328	6.2
17	16967	17486	3.1	16743	17745	6.0
18	18340	18405	0.4	18084	19380	7.2
19	19295	18631	3.4	19077	20283	6.3

Table 1. Natural frequencies and percentage error obtained with 3D and Beam models.

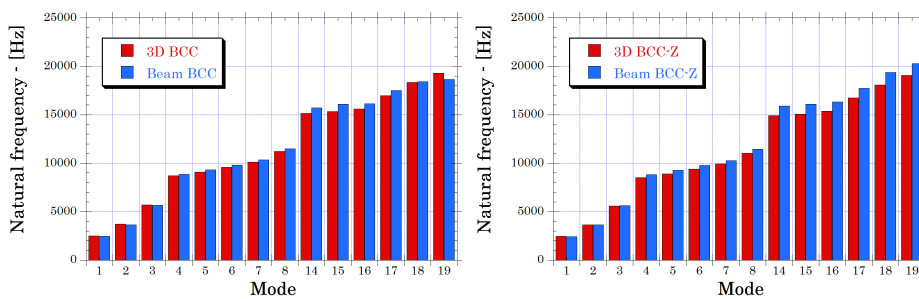

(a) BCC unit cell.

(b) BCC-Z unit cell.

Figure 4. Comparison of frequencies between 3D and Beam elements.

Therefore, in view of the results obtained, it can be considered that the Beam model is validated and will be used from now on to carry out the subsequent analysis.

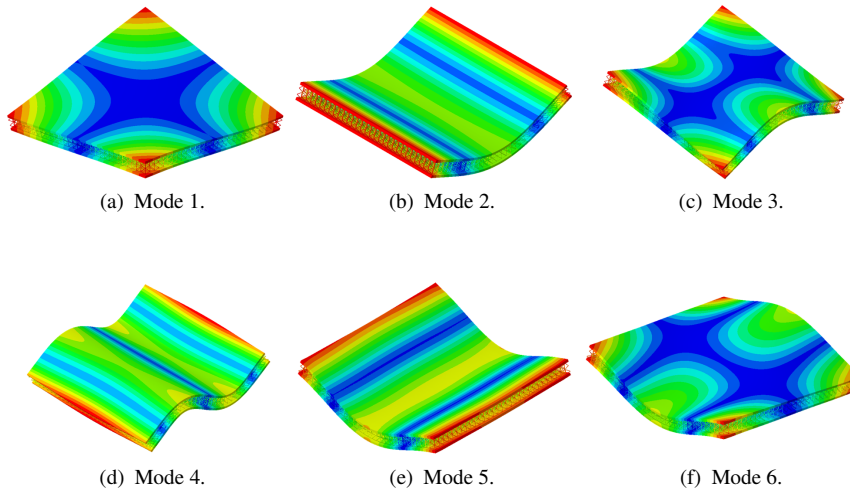

(a) Mode 1. (b) Mode 2. (c) Mode 3.

(d) Mode 4. (e) Mode 5. (f) Mode 6.

Figure 5. Eigenmodes for BCC cell type.

Dynamic analysis of the sandwich structure

In this section, a complete analysis of the dynamic response of the plates is presented, taking into account only those structures with no damage.

As a first result, it can be seen in Fig. 5 the deformed shape for the six first eigenmodes in sandwich structures with ML core of type BCC. It is important to highlight that the eigenmodes for both types of unit cell for the ML core (that is BCC and BCC-Z) are almost identical, showing the corresponding to BCC cell type as an example. Only the first six eigenmodes have been represented because they have the greatest significance in the final deformed shape of the structure, although the first 19 vibration modes have been calculated, as will be corroborated below.

With respect to the values of the natural frequencies of vibration, the results are shown by analyzing the influence of both the unit cell size and type. As previously stated, two different cell topologies have been

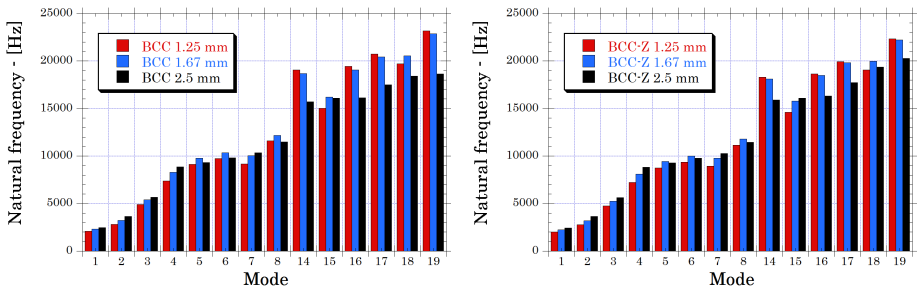

(a) BCC unit cell.

(b) BCC-Z unit cell.

Figure 6. Influence of different cell size.

considered, the BCC and the BCC-Z. In terms of cell size, three different unit cell sizes have been taken into account: 2.5, 1.67 and 1.25 mm.

In Fig. 6 the influence of the cell size can be observed for BCC (Fig. 6(a)) and BCC-Z unit cells (Fig. 6(b)). In both cases, the first nineteen eigenfrequencies have been obtained, omitting those that have a very low probability of appearing. As can be seen, the results for BCC and BCC-Z unit cells are quite similar, with both cases following the same trends. The only cell size for which the natural frequencies of vibration always increase with the eigenmodes is 2.5 mm. On the other hand, for the immediately smaller cell size (1.67 mm.), some decreases are observed when switching from modes 6 to 7 and from 14 to 15. Furthermore, when the smallest size (1.25 mm.) is analysed, a new decay appears when switching from mode 17 to 18.

The results comparing the different cell topologies are shown in Fig. 7, for each of the considered cell sizes. It is important to note here that for small unit cell sizes, the natural frequencies obtained with the BCC cell core topology are always higher than those corresponding to the BCC-Z topology. However, for the largest of the cell sizes considered, this trend is reversed, observing that for high eigenmodes values, the

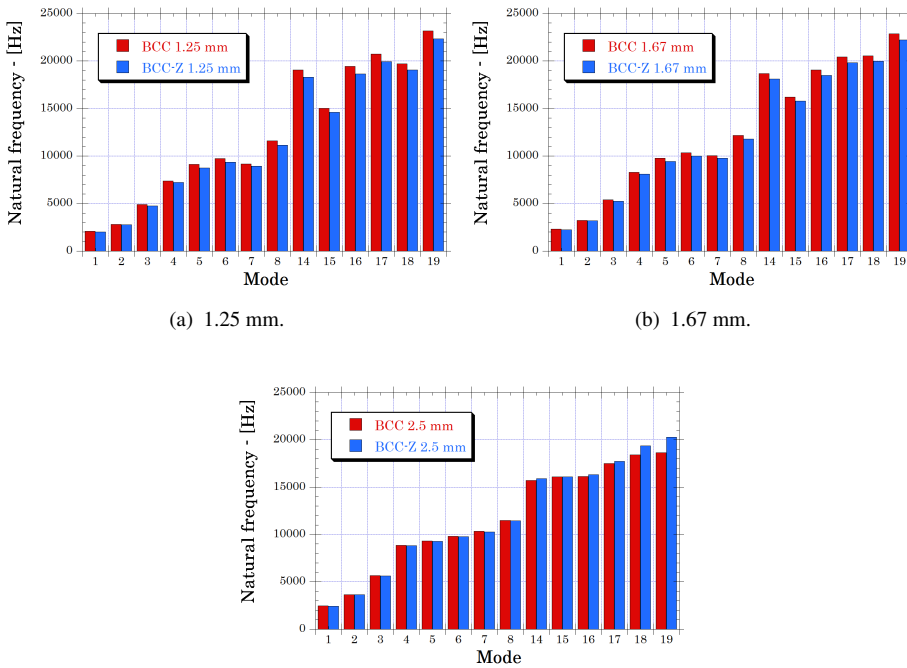

(a) 1.25 mm.

(b) 1.67 mm.

(c) 2.5 mm.

Figure 7. Influence of different cell type.

eigenfrequencies corresponding to the BCC-Z configuration are greater than the corresponding to BCC.

Therefore, as partial conclusions, it can be determined that for small unit cell sizes, the relationship between eigenmodes and the corresponding eigenfrequencies is not always increasing. Furthermore, for these unit cell sizes, the eigenfrequencies in the case of BCC topology are always higher than those for the BCC-Z topology, while for the largest of the considered sizes (2.5 mm), this trend is reversed.

Damage analysis

Effect of damage localisation. The damage in the core of the studied sandwich structures was included using an algorithm implemented in MatLab, which works as follows: after a percentage of damage is selected by the user, the code is executed and programmed to delete a certain number of elements (struts) randomly; thus, for a same percentage of damage, the elements of the core that are removed from the analysis do not necessarily have the same location. As a result, the need to carry out a detailed study of the effect of the damage localisation on the dynamic response of the sandwich structures is readily apparent.

For each eigenmode, the natural frequency was obtained in five simulations with the same damage percentage (from 5% to 40%). Therefore, five values of natural frequency were determined for each case, calculating the Standard Deviation (SD) and the Average Natural Frequency (ANF), which results from averaging the five natural frequencies obtained in this section (same eigenmode and same damage percentage). Variations were analysed in terms of the following ratio:

$$\mathrm{SDV}_i\,(\%) = \frac{\mathrm{SD}_i}{\mathrm{ANF}_i} \cdot 100 \tag{1}$$

where i corresponds to the studied eigenmode.

The SDV ratio as a function of the eigenmode is shown in Fig. 8 for each cell type and cell size. For the sake of brevity and since the variations of natural frequencies are more noticeable at higher damage percentages, only results for a damage of 40% are presented.

Natural frequencies are more sensitive to damage localisation for larger cell sizes, as results for ML with cell size of 2.5 mm presenting more differences in SDV ratio when compared to the ones obtained for cell sizes of 1.25 mm and 1.67 mm. This is due to the way the algorithm operates to produce damage: removing complete elements (struts). In

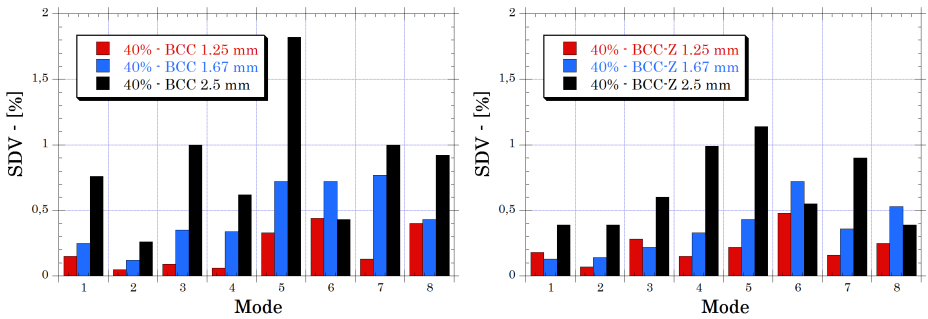

(a) BCC (b) BCC-Z

Figure 8. SDV as a function of eigenmode.

order to reach the same percentage of damage, fewer struts are deleted in the case of cores with cell size of 2.5 mm than in the case of cell sizes of 1.25 mm. This is due to the size of a single strut in each case. However, deleting less struts produce a more localised damage in the structures and, consequently, its influence on the dynamic behaviour of the structure is increased. That is, the larger the cell size, the greater the local effect of damage on the structural response.

In addition, BCC cell type presents more dependence to damage localisation than BCC-Z: although there are similarities between both unit-cells, BCC-Z cells are reinforced with vertical struts (see Fig. 2) that improve the stability of the core and makes it less dependent of damage localisation.

In any case, maximum values for SDV ratio (for eigenmodes 1 to 8) are presented in Table 2, in which maximum variations are below 2% in all cases.

As a conclusion, damage localisation does not affect the natural frequencies of the studied sandwich structures. Therefore, in the following

	Size 1.25 mm		Size 1.67 mm		Size 2.5 mm	
Damage (%)	BCC	BCC-Z	BCC	BCC-Z	BCC	BCC-Z
5	0.07	0.06	0.13	0.19	0.33	0.27
10	0.13	0.16	0.24	0.30	0.29	0.36
15	0.14	0.14	0.35	0.29	0.44	0.58
20	0.12	0.17	0.55	0.34	1.16	0.54
25	0.18	0.20	0.67	0.45	0.68	0.61
30	0.25	0.20	0.61	0.49	1.19	0.96
35	0.42	0.25	0.82	0.45	1.20	1.39
40	0.44	0.48	0.77	0.72	1.82	1.14

Table 2. Maximum SDV as a function of cell size, cell type and damage percentage

sections ANF will be used in the dynamic analysis of core-damaged sandwich structures.

Effect of damage on eigenmodes. In order to study the effect of damage on the eigenmodes of sandwich structures, the normalised natural frequency of damaged structures is presented as a function of the selected eigenmodes in Fig. 9. As the damage localisation was found to have more influence on cores with greater cell size, results of ML core 2.5 mm are selected for the analysis. The natural frequency of damaged sandwich structures has been normalised with respect to the natural frequency of undamaged structures with same cell size and type.

Normalised natural frequencies of damaged structures show greater dependence on the eigenmodes for the case of cores with BCC unit cells than for those with BCC-Z cells. This is due to the reinforcement that BCC-Z cells have with respect to the BCC in the form of a central pillar that add stability, as already explained in the previous section. The maximum differences are 35% and 30% for BCC and BCC-Z cores, respectively.

In general, the trends for both cell types are very similar and the effect of damage in the eigenmodes increases with the percentage of damage. In both cell types, the eigenmode with the most influence on the results

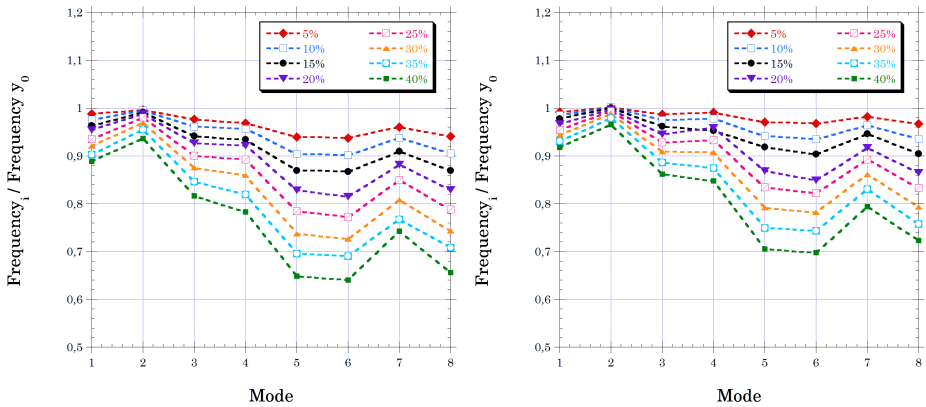

(a) BCC (b) BCC-Z

Figure 9. Normalised frequencies vs damage.

is number 6; thus, results of the following sections will be presented as a function to this eigenmode.

Effect of cell size. In Fig. 10 is shown the effect of the damage on the sandwich structure as a function of the cell size. This figure corresponds to the three sizes studied for both BCC and BCC-Z unit cell types. As stated in the previous section, only results for eigenmode 6 are shown, since it is the eigenmode in which the influence of the damage is more noticeable. Variations are again more visible for results of structures with BCC cells than for BCC-Z.

Natural frequency decrease with increasing percentage of damage for the three sizes. For less damage level, cells of 1.67 mm shows greater frequencies when compared to cells of 2.5 mm and 1.25 mm, However this trend changes when a certain damage level is reached, and cores with cells of smaller size (1.25 mm) present less changes in the natural frequency with the augmenting of damage. The greatest differences are shown for larger cells (2.5 mm), in which the decrease is almost linear with

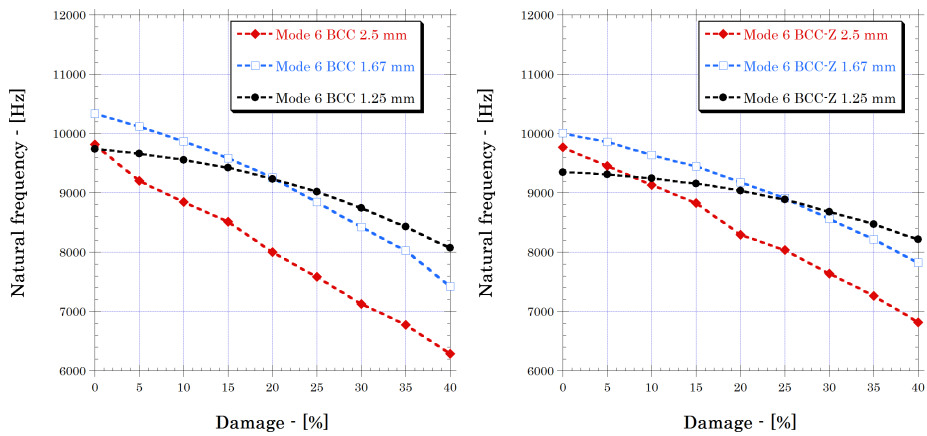

(a) BCC (b) BCC-Z

Figure 10. Frequencies vs damage for different cell sizes.

damage. These results are explained in a similar way to those presented in section 4.3.1: as the level of damage increases, cores with smaller unit cells distribute removed struts more homogeneously. Thus, cores with greater cell sizes are more affected by damage.

Effect of cell type. Comparison of natural frequency as a function of damage for each cell type is shown in Fig. 11. As previously stated, differences between natural frequencies (from undamaged cores to 40% of damage level) are more noticeable in BCC results than in BCC-Z due to their structural arrangement.

Trends are similar for both unit cells. For cell size of 2.5 mm, natural frequencies are always higher for BCC-Z cells; however, for the smallest cell size (1.25 mm), natural frequencies are higher in BCC results up to a damage level of 35%, in which BCC results are slightly lower than BCC-Z. For cell sizes of 1.67 mm, BCC natural frequencies are lower than the ones given for BCC-Z from damage level of 25%.

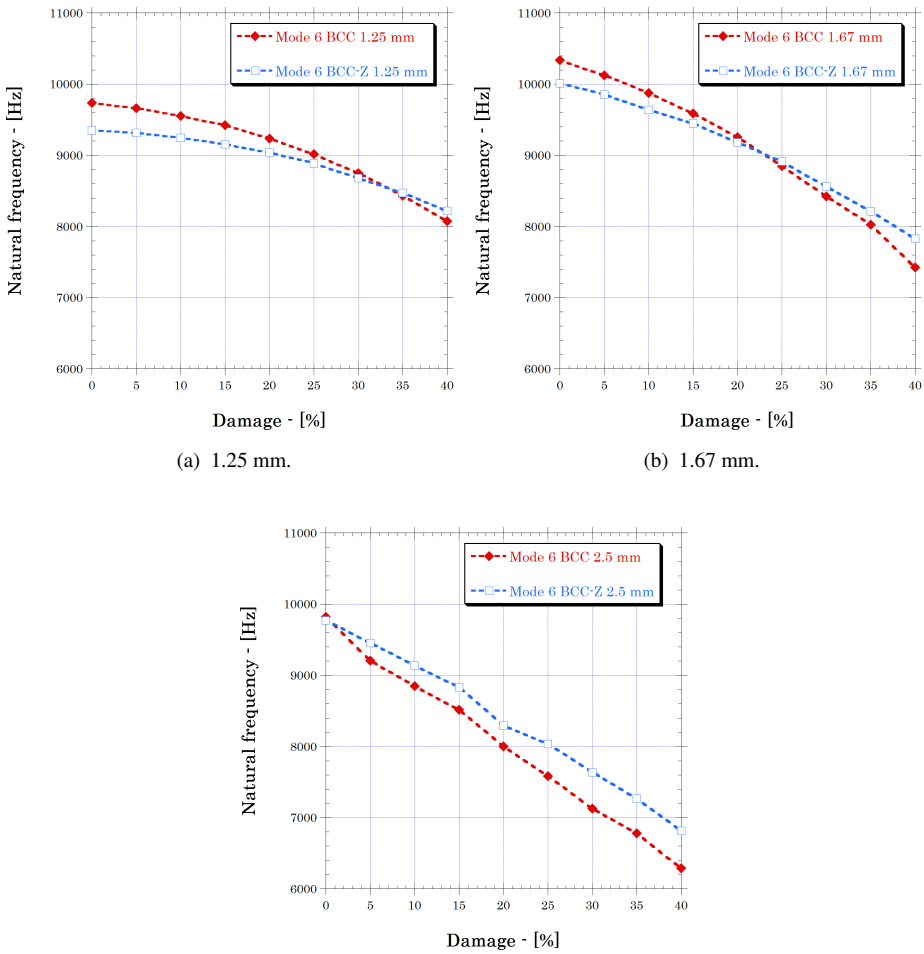

(a) 1.25 mm.

(b) 1.67 mm.

(c) 2.5 mm.

Figure 11. Frequencies vs damage for different cell types.

Effect of cell material types. In order to analyse the effect of the Micro Lattice core material on the free vibration response, it have been considered two simply-supported square plates of approximately the same weight but different ML core materials: stainless steel 316L and Titanium Alloy Ti-6Al-4V[30].

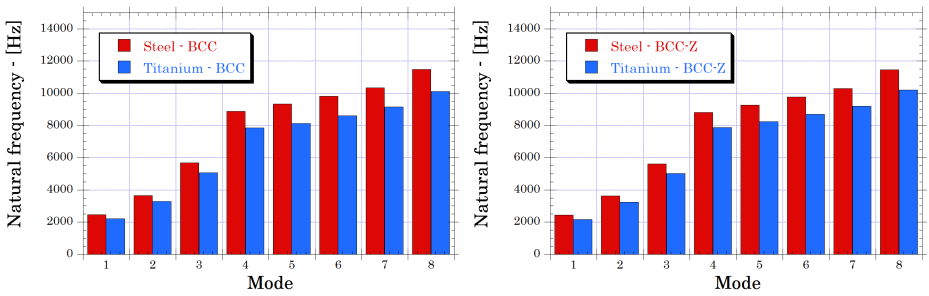

(a) BCC (b) BCC-Z

Figure 12. Natural frequencies for undamaged specimens. Steel vs Titanium cell core.

The mechanical properties of the Ti-6Al-4V used in this analysis are: Young's Modulus $E = 45$ GPa, Poisson's ratio $\nu = 0.30$ and density $\rho = 4680$ kg/m^3 [14].

In this study, only the core cell size of 2.50 mm has been considered, for both cell materials. The diameters of the struts adopted for the ML core of Ti-6Al-4V are 0.35 mm, while for the stainless steel 316L are 0.20 mm, in agreement with the work presented by Mines *et al.* [14].

In first place, the natural frequencies on undamaged sandwich structures have been analysed, for both core materials and for the two typologies previously studied.

Results for both cell types and materials show similarities. As it was presented in previous sections, the natural frequency increases with increasing eingemode number. Natural frequencies for sandwich structures with Titanium micro-lattice core are lower than the obtained for Steel core structures. In general, natural frequency is proportional to the square root of the stiffness (controlled by the Young's Modulus of the material) and inversely proportional to the square root of the mass (controlled by the density). Steel has a Young's Modulus 68% higher than the one given for the Titanium, while its density is just 40% higher;

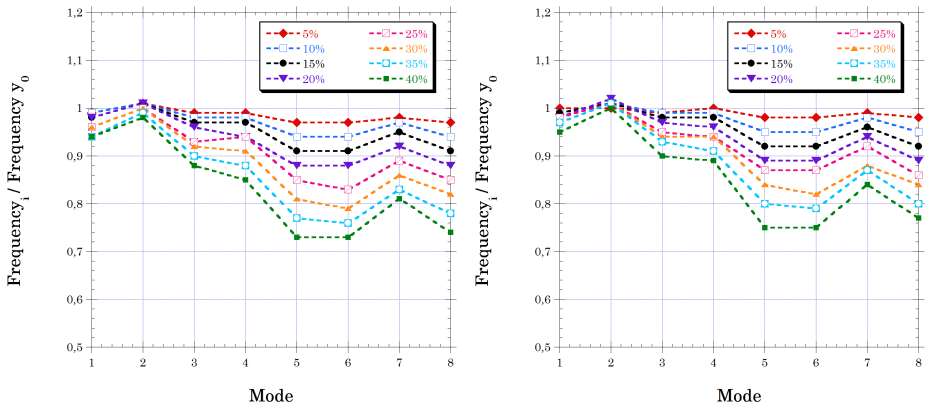

(a) BCC (b) BCC-Z

Figure 13. Normalised frequencies vs damage for Titanium cell core.

therefore, natural frequencies for Steel micro-lattice cores are higher than the ones obtained for micro-lattice cores made of Titanium.

Fig. 13 presents the normalised natural frequency of damaged sandwich structures with Titanium micro-lattice core. For both BCC and BCC-Z cell types, eigenmode number 6 is the more affected by the presence of damage, which coincides with results obtained for Steel cores.

Once the eigenmode that is most affected by the presence of damage has been identified for both materials, a comparison of how damage growth affects the natural frequencies for the two cell types studied as a function of the material is presented in Fig. 10. As previously stated, Steel cores show higher natural frequencies in all cases due to its higher properties, particularly the value of Young's modulus. In BCC structural arrangement, natural frequencies for Steel are more affected by the presence of damage than in the case of Titanium, as differences between the natural frequency without damage (damage of 0%) and natural frequency with a damage level of 40% are 36% and 27% for Steel and Titanium, respectively (Fig. 14 a). For BCC-Z cell type, natural frequencies of Steel and Titanium

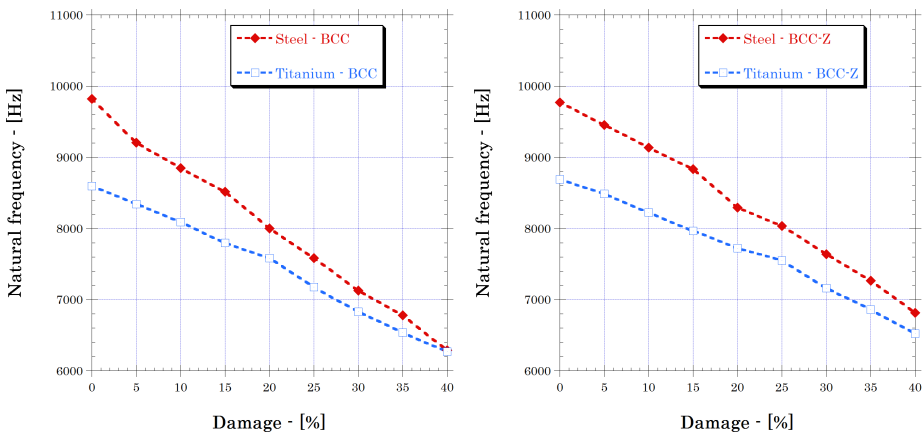

(a) BCC (b) BCC-Z

Figure 14. Frequencies of the eigenmode number 6 vs damage for different cell material.

decrease at a similar rate with augmenting damage level, 30% and 25% respectively. As a conclusion, the dynamic behaviour of BCC-Z micro-lattice cores is less affected by the properties of the material used in its manufacture.

Conclusions

In this work, we implemented a finite element model to study the dynamic frequency responses of sandwich plates with micro-lattice metallic core. The simulations are focused to show the sensitivity of the dynamic responses with the presence of defects in the micro-lattice core. In this way, we developed a MatLab code to generate random defects in the ML core.

We presented an extensive parametric study, where we analysed the effect of: localisation defects, cell sizes, cell types and cell material types. The following points are the principal conclusions from this analysis:

- Natural frequencies are more sensitive to damage localisation for larger cell sizes. Furthermore, the BCC unit cell type presents more dependence to damage localisation than BCC-Z. However, the damage localisation does not affect significantly the natural frequencies of the studied sandwich plates.
- For BCC and BCC-Z cells the effect of damage in the eigenmodes increases with the percentage of damage. In both cell types, the eigenmode with the most influence on the results is number 6.
- The dynamic response of the sandwich structures with greater cell sizes are more affected by damage.
- The natural frequencies present the same tendency for both types of unit cells.
- Natural frequencies for sandwich structures with Titanium micro-lattice core are lower than the obtained for Steel core structures.

Therefore, we could conclude that NDT based on vibration analysis can be an interesting tool to detect the damage of sandwich plates with ML cores. However, future works are required to validate our numerical results with experimental data. Furthermore, we can study the sensitive of the mechanical properties with the presence of defects in micro-lattice blocks.

Acknowledgments

The authors wish to gratefully acknowledge the financial support of the Spanish Ministry of Economy and Competitiveness under Projects DPI2011-24068 and DPI2011-23191.

References

1. Soden PD. Indentation of composite sandwich beams. *The Journal of Strain Analysis for Engineering Design* 1996; 31(5): 353–360.

2. Kamiya N. Analysis of the large thermal bending of sandwich plates by a modified berger method. *The Journal of Strain Analysis for Engineering Design* 1978; 13(1): 17–22.
3. Holt PJ and Webber JPH. Exact solutions to some honeycomb sandwich beam, plate, and shell problems. *The Journal of Strain Analysis for Engineering Design* 1982; 17(1): 1–8.
4. Udatha P, Kumar CVS, Nair NS et al. High velocity impact performance of three-dimensional woven composites. *The Journal of Strain Analysis for Engineering Design* 2012; 47(7): 419–431.
5. Vinson J. *The behavior of sandwich structures of isotropic and composite materials*. Routledge, 2018.
6. Heimbs S, Cichosz J, Klaus M et al. Sandwich structures with textile-reinforced composite foldcores under impact loads. *Composite structures* 2010; 92(6): 1485–1497.
7. Lolive É and Berthelot JM. Non-linear behaviour of foam cores and sandwich materials, part 2: indentation and three-point bending. *Journal of Sandwich Structures & Materials* 2002; 4(4): 297–352.
8. Berthelot JM and Lolive É. Non-linear behaviour of foam cores and sandwich materials, part 1: Materials and modelling. *Journal of Sandwich Structures & Materials* 2002; 4(3): 219–247.
9. Sypeck DJ. Cellular truss core sandwich structures. *Applied Composite Materials* 2005; 12(3-4): 229–246.
10. Queheillalt DT and Wadley HN. Titanium alloy lattice truss structures. *Materials & Design* 2009; 30(6): 1966–1975.
11. Rashed M, Ashraf M, Mines R et al. Metallic microlattice materials: A current state of the art on manufacturing, mechanical properties and applications. *Materials & Design* 2016; 95: 518–533.
12. Gümrük R, Mines R and Karadeniz S. Static mechanical behaviours of stainless steel microlattice structures under different loading conditions. *Materials Science and Engineering: A* 2013; 586: 392–406.
13. Tsopanos S, Mines R, McKown S et al. The influence of processing parameters on the mechanical properties of selectively laser melted stainless steel microlattice structures. *Journal of Manufacturing Science and Engineering* 2010; 132(4): 041011.
14. Mines R, Tsopanos S, Shen Y et al. Drop weight impact behaviour of sandwich panels with metallic micro lattice cores. *International Journal of Impact Engineering* 2013; 60: 120–132.
15. Jacobsen AJ, Barvosa-Carter W and Nutt S. Compression behavior of micro-scale truss structures formed from self-propagating polymer waveguides. *Acta Materialia* 2007; 55(20): 6724–6733.

16. Cansizoglu O, Harrysson O, Cormier D et al. Properties of ti–6al–4v non-stochastic lattice structures fabricated via electron beam melting. *Materials Science and Engineering: A* 2008; 492(1-2): 468–474.
17. Hasan R, Mines R and Tsopanos S. Determination of elastic modulus value for selectively laser melted titanium alloy micro-struty. *Journal of Mechanical Engineering and Technology (JMET)* 2010; 2(2).
18. Doebling SW, Farrar CR, Prime MB et al. Damage identification and health monitoring of structural and mechanical systems from changes in their vibration characteristics: a literature review. Technical report, Los Alamos National Lab., NM (United States), 1996.
19. Yang Z, Wang L, Wang H et al. Damage detection in composite structures using vibration response under stochastic excitation. *Journal of Sound and Vibration* 2009; 325(4): 755 – 768.
20. Kwon Y and Lannamann D. Dynamic numerical modeling and simulation of interfacial cracks in sandwich structures for damage detection. *Journal of Sandwich Structures & Materials* 2002; 4(2): 175–199.
21. Duc ND, Cong PH, Tuan ND et al. Nonlinear vibration and dynamic response of imperfect eccentrically stiffened shear deformable sandwich plate with functionally graded material in thermal environment. *Journal of Sandwich Structures & Materials* 2016; 18(4): 445–473.
22. Saraswathy B, Mangal L and Kumar RR. Analytical approach for modal characteristics of honeycomb sandwich beams with multiple debond. *Journal of Sandwich Structures & Materials* 2012; 14(1): 35–54.
23. Elmalich D and Rabinovitch O. On the effect of inter-laminar contact on the dynamics of locally delaminated frp strengthened walls. *International Journal of Non-Linear Mechanics* 2015; 77: 141 – 157.
24. Zou Y, Tong L and Steven G. Vibration-based model-dependent damage (delamination) identification and health monitoring for composite structures — a review. *Journal of Sound and Vibration* 2000; 230(2): 357 – 378.
25. Farrar CR and Worden K. An introduction to structural health monitoring. *Philosophical Transactions of the Royal Society of London A: Mathematical, Physical and Engineering Sciences* 2007; 365(1851): 303–315.
26. ABAQUS/Standard. *Abaqus Standard v6.13 User's Manual*. version 6.13 ed. Richmond, USA: ABAQUS Inc., 2013.
27. Burlayenko VN and Sadowski T. Influence of skin/core debonding on free vibration behavior of foam and honeycomb cored sandwich plates. *International Journal of Non-Linear Mechanics* 2010; 45(10): 959–968.

28. Ushijima K, Cantwell W, Mines R et al. An investigation into the compressive properties of stainless steel micro-lattice structures. *Journal of Sandwich Structures & Materials* 2011; 13(3): 303–329.
29. Smith M, Guan Z and Cantwell W. Finite element modelling of the compressive response of lattice structures manufactured using the selective laser melting technique. *International Journal of Mechanical Sciences* 2013; 67: 28–41.
30. Polmear I. *Light alloys: from traditional alloys to nanocrystals*. Elsevier, 2005.